Journal of Physics Communications

OPEN ACCESS

RECEIVED
6 January 2020

REVISED
20 March 2020

ACCEPTED FOR PUBLICATION
24 March 2020

PUBLISHED
7 April 2020

Original content from this work may be used under the terms of the Creative Commons Attribution 4.0 licence.

Any further distribution of this work must maintain attribution to the author(s) and the title of the work, journal citation and DOI.

PAPER

A flexible tactile sensor using seedless hydrothermal growth of ZnO nanorods on fabrics

Gwang-Wook Hong[1,2], **Jihyun Kim**[2], **Jun-Soo Lee**[1,2], **Kyeongho Shin**[1,2], **Dongsoo Jung**[1] and **Joo-Hyung Kim**[1,2]

[1] Department of Mechanical Engineering, Inha University, Incheon, 22212, Republic of Korea
[2] INHA Institute of Space science and Technology (INHA IST), Inha University, Incheon, 22212, Republic of Korea

E-mail: joohyung.kim@inha.ac.kr

Keywords: ZnO, seedless, hydrothermal, nanorods, fabric, electromechanical sensor

Abstract

A flexible and cost-effective electromechanical device for tactile sensing based on ZnO nanorods (ZnO NRs) grown on fabrics is developed. Sensing performance and the electromechanical properties of ethylcellulose/polyurethane-coated ZnO NRs on fabric substrates were tested by the LCR meter, force transducer, vibrator, and pulse analyzer. The peak-to-peak output voltage at an applied force of 21.5 N dropped considerably for the wool-, nylon-, and PP substrates and reached to the order of 3.84 mV, 1.8 mV and 4.1 mV, respectively. Furthermore, the frequency dependency of the dissipation factors revealed abrupt changes at low frequencies, while these changes were negligible at high frequencies.

1. Introduction

Zinc oxide (ZnO) is one of the most promising functional materials due to its remarkable properties such as wide band-gap(~3.37 eV) [1], excellent chemical and thermal stability, piezoelectricity, and so on [2–8]. Since zinc oxide nanorods (NRs) were firstly investigated to be used as a piezoelectric generator, piezoelectric or triboelectric generators for mechanical energy harvesting application has been growing [9]. Recently, new observation as a novel triboelectric generator has been suggested with various structures and rather simple processes [10]. Wearable sensing devices utilizing ZnO NRs structures using these electrical characteristics have been developed in various research fields such as pulse measurement and bending angle measurement [11–13].

In particular, it is reported that one-dimensional (1D) ZnO NRs/nanowires (NWs) are a more suitable structure to possess higher electromechanical coupling and better piezoelectricity due to their larger surface over volume ratios [14, 15]. Also, the 1D ZnO NRs can be easily synthesized using the various chemical as well as physical methods.

Among these fabrication processes, a hydrothermal growing method of ZnO NRs is the most favorable one owing to its flexibility on the growth process with different substrates and even allow to be grown at low process temperatures, which is a simple, cost-effective, scalable, and suitable way to fabricate the uniform ZnO NRs on flexible substrates [16–18]. Also, well-aligned structure of ZnO nanorods has great potential to be developed for sensing applications. Nowadays, wearable or stretchable devices fabricated on flexible substrates have been widely studied and suggested for smart healthcare devices for patient monitoring. However, fabric-based a tactile sensor still needs to be developed with smart nanostructured sensing materials without external power.

Skin tactile sensors are excited by different external stimuli of the human brain and the human nervous system can encode the information acquired by tactile sensors and give different sensations such as pressure, heat, cold, vibrations, and so on. The attempt to create an artificial skin or electronic skin (e-skin) and a skin-like tissue that can simulate the sensitive behavior of human skin is motivated by the possibility of fabricating a multi-sensitive interface for different kinds of applications, such as robotics and prosthetics. In particular, considerations for the development of pressure sensors include pressure range (<20 N), operating frequency (~1 kHz) and reaction time (~1 ms) [19–21]. Therefore, in this study, we would like to fabricate the self-operated tactile sensor on fabric substrates. To achieve this goal, the growth of ZnO seed layer is essential to

© 2020 The Author(s). Published by IOP Publishing Ltd

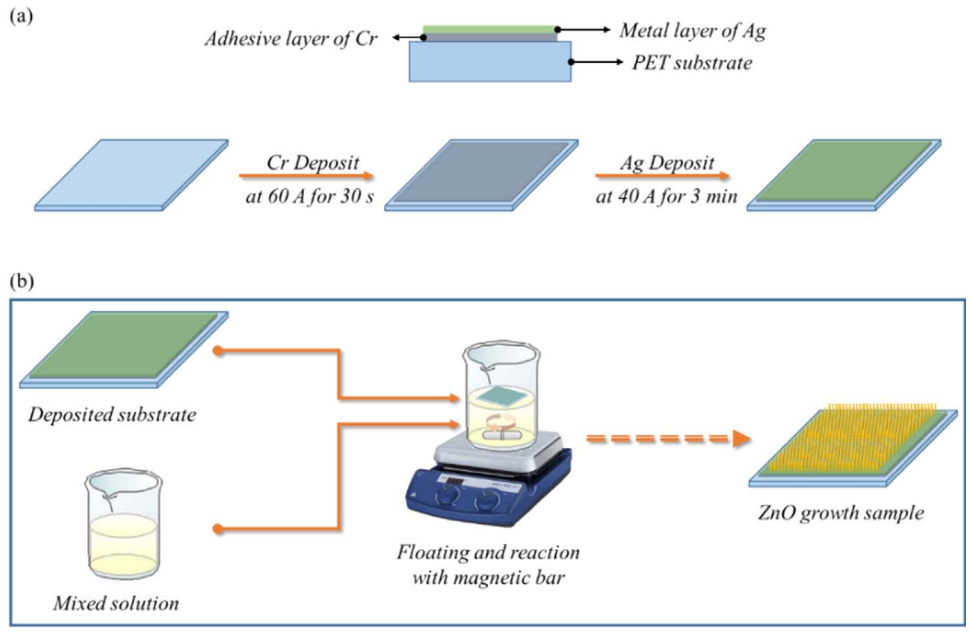

Figure 1. Schematics of (a) deposition process of Cr and Ag double layer and (b) ZnO NRs growth process on fabric substrates.

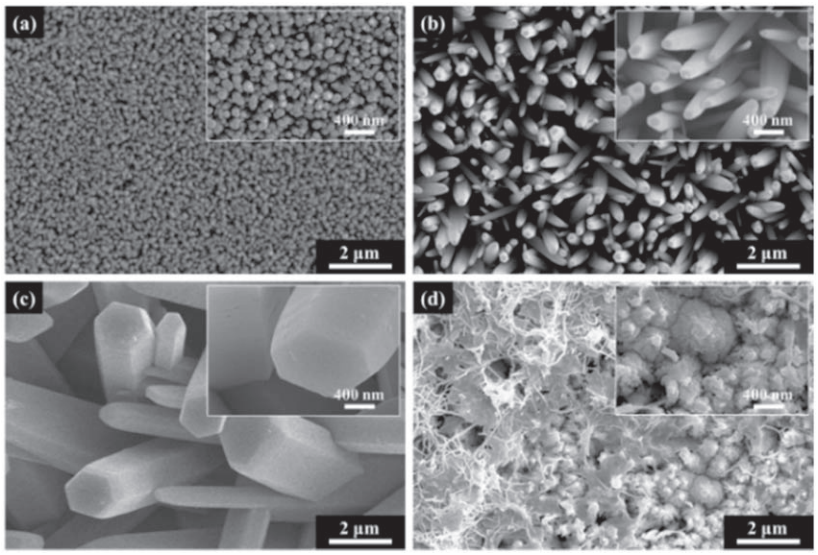

Figure 2. Variation of surface morphology of ZnO NRs grown on PET substrate; NH_4OH (a) 0.5 w.t% , (b) 1.0 w.t% (c) 2.0 w.t% and (d) 3.0 w.t%.

facilitate nucleation and subsequent growth of ZnO NRs, processing at high temperature. However, it can be a hurdle to select the substrates. This process can also allow some impurities during the crystal growth, eventually influencing the adhesion between ZnO nanostructures and underlying substrates [22–28]. To solve the above issue, a seedless hydrothermal method processed at the low temperature can be the solution to successfully grow ZnO NRs on various flexible substrates such as natural and synthetic fabrics. For these approaches in this study, Wool, nylon, and Polypropylene (PP) fabric were selected as flexible substrates for developing portable and wearable electromechanical sensors.

2. Experiment details

Figure 1(a) depicts a schematic process of ZnO NRs growth by a hydrothermal method. In particular, a seedless hydro-thermal growth of ZnO NRs on various natural (cotton, wool) and synthetic (nylon, PP) fabric substrates.

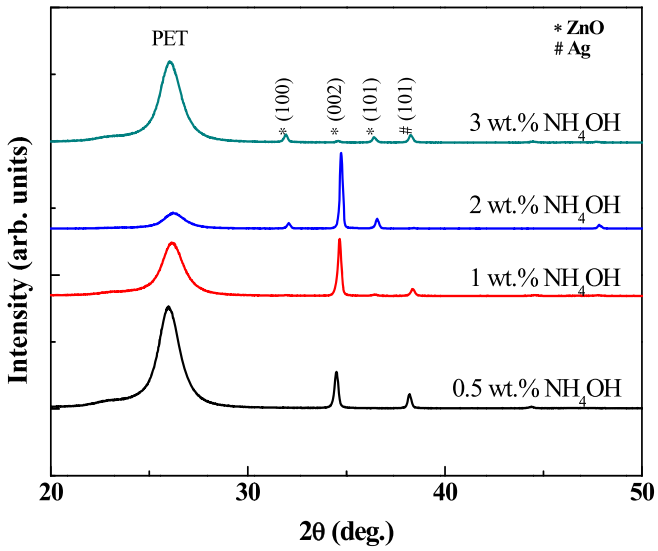

Figure 3. Comparative XRD $\theta-2\theta$ patterns of ZnO NRs grown on PET substrate grown under different NH_4OH concentrations.

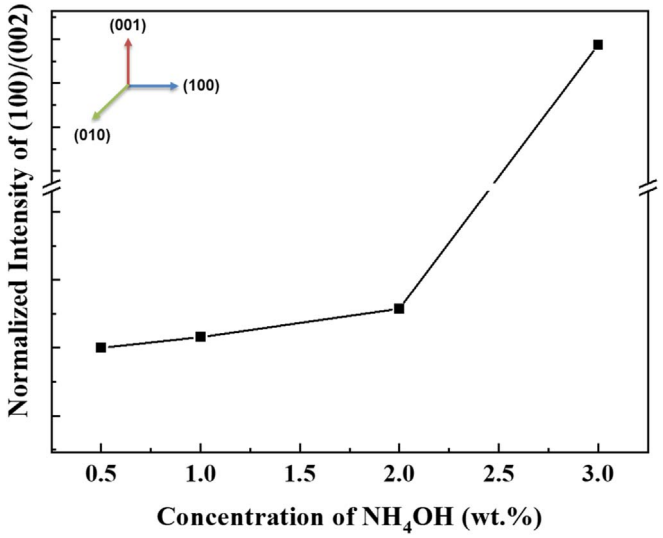

Figure 4. Normalized peak intensity of (100)/(002) as a function of NH_4OH concentration.

To achieve the seedless hydrothermal approach, we selected two metals (Cr, Ag) and deposited on the fabric substrates in the form of thin film by a thermal evaporator. In order to grow ZnO, Ag metal layer is required as a seeding and metallic layer on fabric in this experiment [29]. To minimize delamination, Cr layer is also added an adhesive layer for the metallic layer. Cr plays a role to enhance adhesion between Ag and the substrates. The deposition rates of Cr and Ag were found out to be 120.0 Å min^{-1} and 13.3 Å min^{-1}, respectively. Ag uses to a seed layer, the dissolved Zn^{2+} cations reacted with the OH^- anions to form ZnO precipitates in the reaction solution, the OH^- ions would bind to the Ag surface to form Ag–OH bonds because the oxidation potential of Ag is relatively high. Prior to the deposition, the substrates were cleaned by ethanol and DI-water, followed by drying in an oven at 100 °C for 2 h.

A mixture of deionized water, zinc nitrate hexahydrate ($Zn(NO_3)_2$•$6H_2O$, 98%, reagent grade, Sigma Aldrich), and ammonium hydroxide (NH_3•H_2O, 28%–30% w.t%, reagent grade, Sigma Aldrich) were used as a precursor solution for the growth. The metal-coated substrates were immersed in the precursor solution. During the process, the mixture kept a constant concentration of $Zn(NO_3)_2 \cdot 6H_2O$ at 20 mM while the concentration of $NH_3 \cdot H_2O$ was varied in figure 1(b).

To optimize the growth parameters, the following factors need to be controlled: growth temperature, growth time, precursor concentration, and so on. The growth process of the ZnO NRs involves the chemical reactions mentioned below: [2]

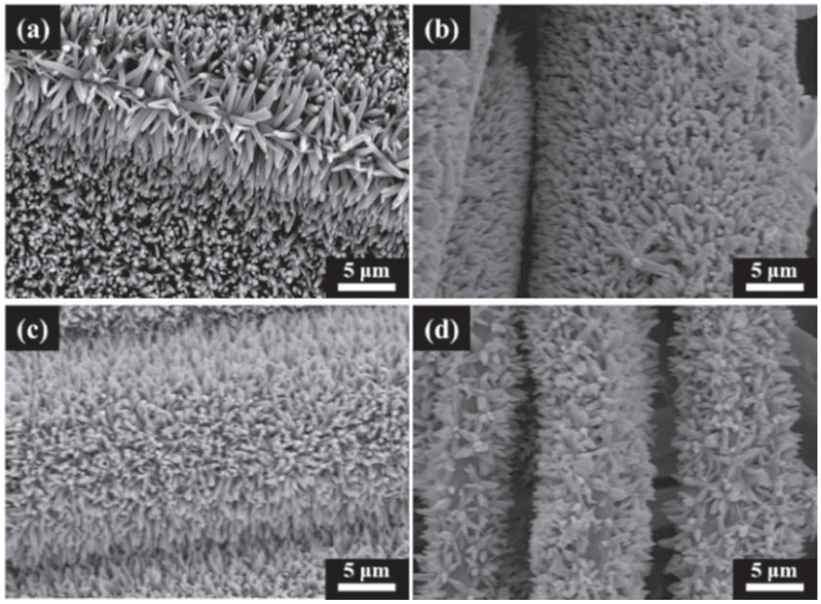

Figure 5. SEM images of ZnO NRs grown under 1.0 wt% NH_4OH concentration on (a) PET, (b) wool, (c) nylon and (d) PP substrates.

$$NH_3 \cdot H_2O \leftrightarrow NH_4^+ + OH^-$$

$$NH_3 \cdot H_2O \leftrightarrow NH_3 \uparrow + H_2O$$

$$Zn^{2+} + 2OH^- \leftrightarrow Zn(OH)_2 \downarrow$$

$$Zn(OH)_2 + 4NH_3 \cdot H_2O \leftrightarrow Zn(NH_3)_4^{2+} + 4H_2O + 2OH^-$$

$$Zn(OH)_2 \leftrightarrow ZnO + H_2O$$

The substrates were placed facing down and kept floating on the surface of the precursor solution inside a double boiler. For optimal ZnO growth based on ammonia concentration, the solution was reacted at 90 °C for 5 h, and the magnetic stirring method was used to prevent the local growth of ZnO NRs. After completing the growth process, the substrates were washed with deionized water and dried at room temperature. To optimize the growth parameters, a systematic investigation was performed by controlling growth temperature and time, and precursor concentration.

The phase purity and crystallinity of the ZnO NRs were examined by x-ray diffractometer (DMAX 2500, Rigaku) using a Cu source ($K\alpha = 1.54056$ Å) and surface morphology was investigated by field-emission scanning electron microscopy (FE-SEM).

The electromechanical properties of the as-grown ZnO NRs/fabric substrates were examined by LCR meter, force transducer, vibrator, and pulse analyzer. Then the device was fabricated by connecting thin copper wires to the substrates using a silver paste, followed by coating polymers (ethylcellulose or polyurethane) for protecting and insulating the as-grown sample surfaces. The intrinsic electrical properties were investigated by measuring impedance and D-factor induced in the substrates. The intrinsic electrical properties of the device were performed by an LCR meter (HP 4284 A). Piezoelectric properties were investigated by a force transducer, vibrator, and pulse analyzer via measuring output voltages induced by applied forces.

Doing so, the device was placed on the upper part of the force transducer where generates the signal in voltage. A square-wave-formed voltage signal was generated from a function generator (Agilent, 33220 A) and applied to a vibrator-knocked rigid body fixture with a force transducer. A data acquisition system (PULSE, B&K) was converted to set the input force control. The voltage signal generated from the devices was also transmitted to the data acquisition system. The vibration was fixed at 3 Hz, 100 mV, and a square wave input from the function generator. The input force of the devices, which was measured by a force transducer, was manually controlled.

3. Results and discussion

Prior to the growth of ZnO NRs on fabric substrates, a flat PET film was used as a test substrate to optimize the growth parameters. The representative SEM images of ZnO NRs are shown in figure 2, revealing the effects of

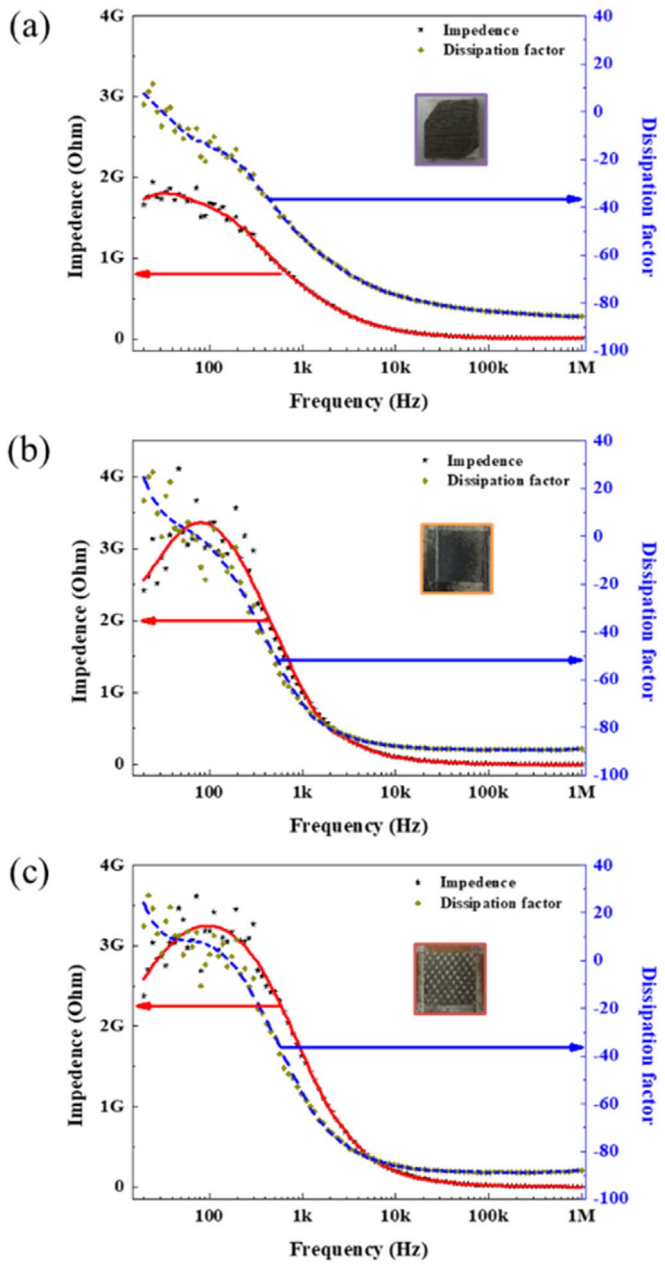

Figure 6. Impedance and D-factor obtained from (a) wool, (b) nylon, and (c) PP-based device.

ammonium concentration (0.5 to 2.0 wt%) on the surface morphology. As the ammonium concentration increases up to 2.0 wt%, the overall dimension of ZnO NRs increases. However, the formation of ZnO NRs was drastically reduced above 2.0 wt% of the ammonium concentration.

X-ray diffraction (XRD) $\theta-2\theta$ pattern of the ZnO NRs grown on PET is shown in figure 3. All the diffraction peaks can be indexed as the hexagonal wurtzite phase of ZnO as reported in the standard card (JCPDS card No. 36–1451) [26]. The intensity of (002) peak is higher than all other peaks, indicating the preferential *c*-axis orientation of the nanorods. Besides, a peak from the PET substrate is also observed at 26.04°. The preferential *c*-axis orientation is strongly related to the ammonium concentration. In figure 4 show the detailed crystal peaks by a ratio of the c-dir. and others.

The morphology of the ZnO NRs on different fabrics was observed by SEM. A very thin ZnO nanorods layer formed on the different types of surfaces. Figure 5 shows the measured SEM images of ZnO NRs on PET, wool, nylon and PP substrates with ZnO NRs at low magnification. In the fabric growth by ZnO NRs indicates the formation of compact, hexagonal-like shape and homogeneously distributed thin nanorods layer on the fabric surface. From the SEM images, it was clear that ZnO NRs were homogeneously distributed over the fabric surface.

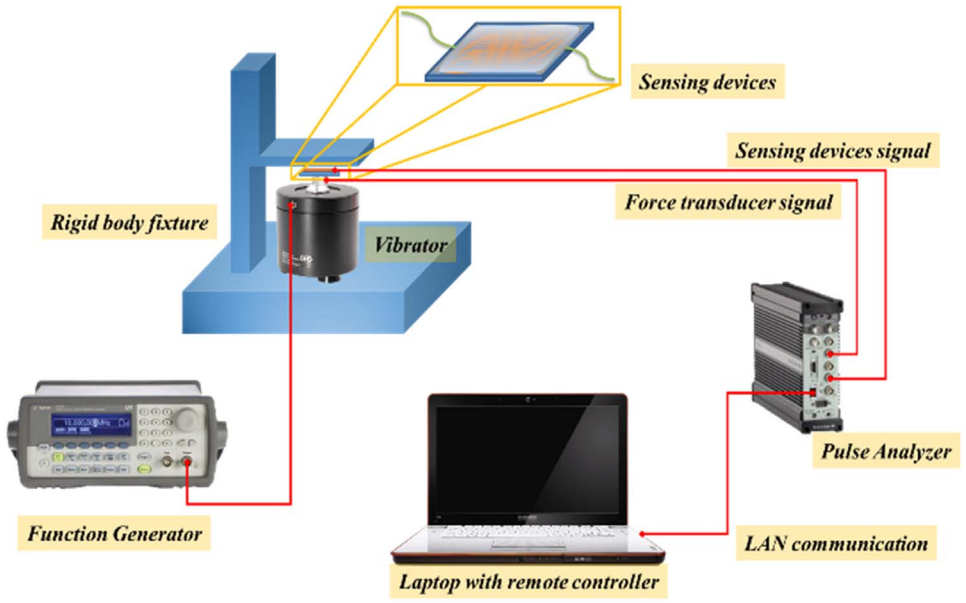

Figure 7. Testing setup for ZnO NRs based tactile sensors.

To investigate feasibility of the prepared fabric substrates as electromechanical portable and wearable sensors, we measured impedance and dissipation-factor (D-factor) of the fabricated fabric-based devices (wool, nylon, PP) because D-factor is an important parameter evaluated in the development of electromechanical sensing devices. The dissipation factor, D, is a measure of energy lost during the reversal of electric polarization and related directly to the measured angular frequency as follows:

$$\mathrm{D} = \frac{R_s}{|X_s|} = R_s C_s \omega$$

where, R_s is the series resistance of the device, C_s is the series capacitance, and ω is the angular frequency.

Figure 6 shows the impedance and D-factor obtained from the wool-, nylon-, and PP-based device. The measurements were performed by sweeping the frequency from 20 Hz to 1 MHz. The *D* value of the PP-based device shows the highest value than other fabric substrates. The piezoelectric signal from ZnO NRs should be analyzed by impedance measurement, which can identify the resistive part and capacitive part. Dissipation is very important to consider the tactile sensor as a piezoelectric induced power without an external power to operate sensors [30].

Over 1 kHz, the D-factor was abruptly changed in all structures on different fabric substrates. However, no significant change in the D-factor in high frequency range is observed. The output signal according to the applied force of the device was evaluated using a vibration generator and a load cell monitoring system. As shown in figure 7, the applied force of the sensor was controlled by the vibration cycle of the vibration generator. To investigate the electromechanical properties for the maximum fingertip force, approximately 20 N was repeatedly applied at a 3 Hz cycle to each sensing device.

Figure 8 shows the voltage induced by the applied force. As seen in figure 8, the resultant peak-to-peak output voltage (V_{PP}) is 3.84 mV, 1.8 mV, and 4.1 mV, in the wool-, nylon-, and PP-based device, respectively. The output voltage depends on applied forces. The line signals fitted by Fast Fourier Transform (FFT) can be seen in figure 8(b).

The difference in the output voltages might be caused by elasticity originated from the substrate's intrinsic properties. As such, PP has a higher elastic modulus compared to wool and nylon. The relatively high V_{pp} observed in the PP-based device can be deduced from the applied force-time curve in figure 8(a). The obtained curves from the wool- and PP-based device imply that the applied force acted on the devices was slowly released and left a residual force behind when the applied force was removed. The residual force may enhance to produce output voltages. However, a more detailed investigation will be needed for clarifying the effects of the substrate's elastic modulus on output voltages.

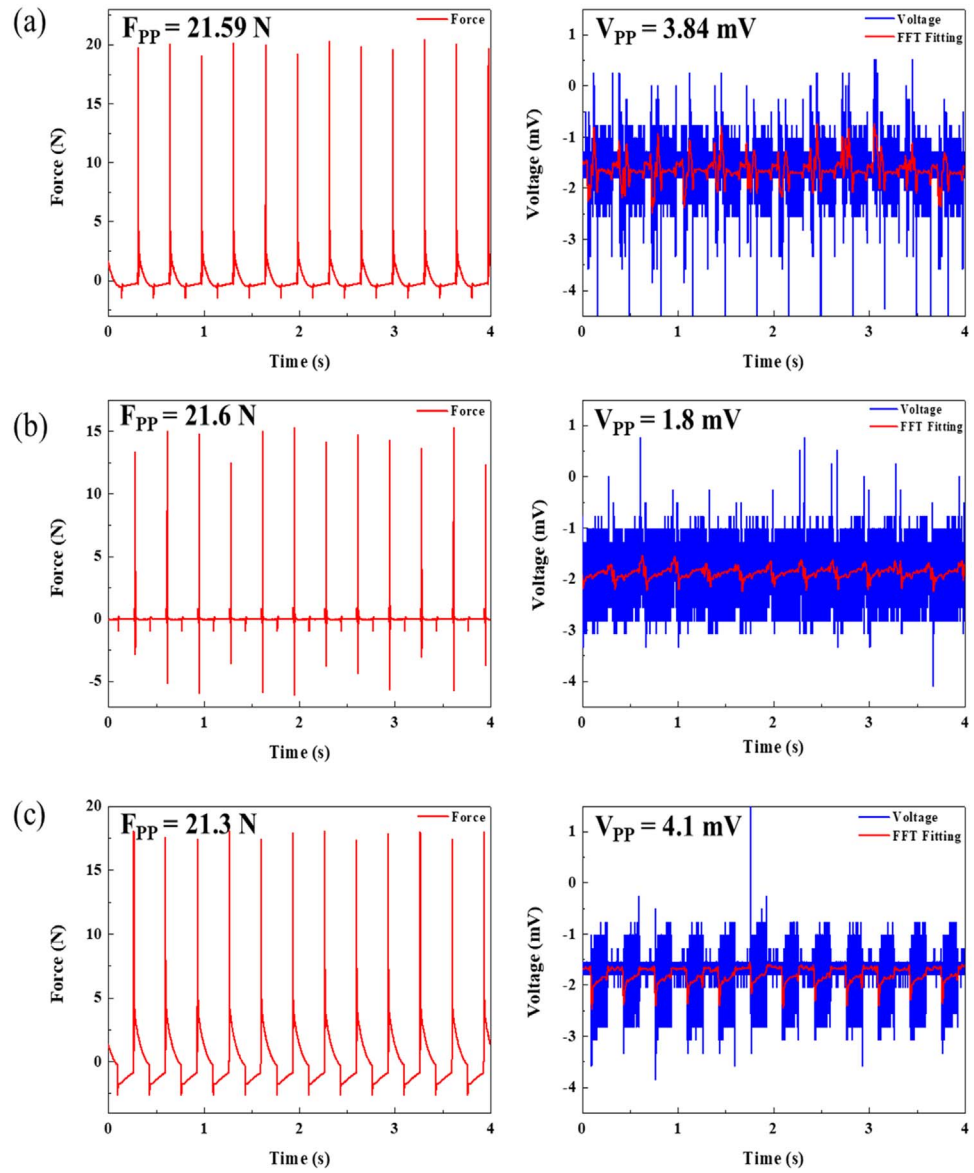

Figure 8. Applied force and the resultant output voltage of each device (a) wool, (b) nylon, and (c) PP-based device.

4. Conclusions

We fabricated a simple electro-mechanical ZnO NRs sensing device on natural and synthetic fabric substrates. ZnO NRs were grown on wool, nylon, and PP fabric substrates at low temperature by a seedless hydrothermal method. The crystallographic growth of c-directional oriented ZnO NRs was controlled by growth temperature and time, precursor concentrations. We tested the basic experiments only with various bare fabrics, however, the measured data include dominant noise, resulting in no significant signal output from experiments.

The feasibility of detection by cyclic impact for a sensing device for health monitoring application was tested. Based on the measurement, lower frequency range (<100 Hz) will be expected for tactile sensor operation frequency because the ZnO NRs on fabric shows more dominant resistive behavior with low dissipation. The obtained peak-to-peak output voltage (V_{PP}) under an applied force of 21.5 N was 3.84 mV, 1.8 mV, and 4.1 mV, in the wool-, nylon-, and PP-based device, respectively. Furthermore, it is observed that the dissipation factors are greatly changed in the low frequency range while a negligible change in the high frequency range.

From this experiment, this new type of flexible sensor applications using nano-rod ZnO structure grown on fabric as a feasible of sensors for medical applications such as wearable fabric sensors.

Acknowledgments

This work was supported by a grant funded by INHA university (2019).

ORCID iDs

Gwang-Wook Hong https://orcid.org/0000-0003-3689-781X

References

[1] Heo N, Tien K, Kang R and Pearton L R 2004 *Materials Science and Engineering R* **47** 1–47
[2] Wen W and Ding W 2012 *Journal of Materials Chemistry* **22** 9469–76
[3] Wang Y X, Liu S, Lai L X and Gao S R 2009 *Chinese Science Bulletin* **54** 14–18
[4] Dem'yanets L N, Kuz'mina D V and Kuz`mina I P 2002 *Inorganic Materials* **38** 124–31
[5] Xu S, Qin Y, Xu C, Wei Y and Wang Z L 2010 *Nature Nanotechnology* **5** 366–73
[6] Law M, Greene L E, Johnson J C, Saykally R and Yang P 2005 *Nature Materials* **4** 455–9
[7] Xu S, Xu C, Liu Y, Hu Y, Yang R, Yang Q, Ryou J H, Kim H J, Lochner Z, Choi S, Dupuis R and Wang Z L 2010 *Advanced materials* **22** 4749–53
[8] Wang Z L 2010 *The Journal of Physical Chemistry Letters* **1** 1388–93
[9] Chandrasekaran S, Bowen C, Roscow J, Zhang Y, Dang D K, Kim E J, Misra R D K, Deng L, Chung J S and Hur S H 2019 *Physics Reports* **792** 1–33
[10] Al-Ruqeishi M S, Mohiuddin T, Al-Habsi B, Al-Ruqeishi F, Al-Fahdi A and Al-Khusaibi A 2019 *Arabian Journal of Chemistry* **12** 5173–9
[11] Lee T, Lee W, Kim S-W, Kim J J and Kim B-S 2016 *Advanced Functional Materials* **26** 6206–14
[12] Shin K Y, Lee J S and Jang J 2016 *Nano Energy* **22** 95–104
[13] Hemtej Gullapalli V S M, Vemuru A, Kumar, Andres Botello-Mendez R, Vajtai M, Terrones S, Nagarajaiah and Ajayan P M 2010 *Small* **6** 1641–6
[14] Vaibbina P K, Kaushik A, Pokhrel N., Bhansali S and Pala N 2015 *Biosensors and Bioelectronics* **15** 124–30
[15] Han C, Zhang C, Zhang N, Colmenares J C and Xu Y J 2014 *Advanced Functional Materials* **25** 221–9
[16] Zhao S, Shen Y, Yan Xi, Zhou P, Yin Y, Lu R, Han C, Cui B and Wei D 2019 *Sensors and Actuators B: Chemical* **286** 501–11
[17] Hoa L T, Tien H N and Hur S H 2014 *Sensors and Actuators A: Physical* **207** 20–4
[18] Lee James S, Shin K Y, Cheong O J, Kim J H and Jang J S 2015 *Scientific Reports* **20** 7887–95
[19] Greene L E, Law M, Goldberger J, Kim F, Johnson Justin C, Zhang Y, Saykally R J and Yang P 2003 *Angewandte Chemie International Ed.* **42** 3031–4
[20] Li Q, Kumar V, Li Y, Zhang H, Marks T J and Chang P H 2005 *Chemistry of Materials* **17** 1001–6
[21] Scarpellini D, Paoloni S, Medaglia P G, Pizzoferrato R, Orsini A and Falconi C 2015 *Materials research bulletin* **65** 231–7
[22] Fan H J, Fleischer F, Lee W, Nielsch K, Scholz R, Zacharias M, Gosele U, Dadgar A and Krost A 2004 *Superlattices and Microstructures* **34** 95–105
[23] Willander M, Nur O, Zhao Q X, Yang L L, Lorenz M, Cao B Q, Perez J Z, Czekalla C, Zimmermann G, Grundmann M, Bakin A, Behrends A, Al-Suleiman M, El-Shaer A, Mofor A C, Postels B, Waag A, Boukos N, Travlos A, Kwack H S, Guinard J and Dang D L S 2009 *Nanotechnology* **20** 1–40
[24] Li X, Zhou Xin, Wang C, Liu J, Sun P, Liu F and Lu G 2014 *Applied Materials & Interfaces* **6** 18661–7
[25] Viola Fabrizio A and Cosseddu Pierro 2018 *Sensors for Diagnostics and Monitoring* (Boca Raton, FL: CRC Press) 149–174 (https://www.taylorfrancis.com/books/e/9781351250092)
[26] Cole K J 2006 *Experimental Brain Research* **175** 285–91
[27] Valero-Cuevas F J 2000 *Journal of Neurophysiology* **83** 1469–79
[28] Li G, Wu X and Lee D-W 2015 *Sensors and Actuators B: Chemical* **221** 1114–9
[29] Chiou W T, Wu W Y and Ting J M 2003 *Diamond and Related Materials* **12** 1841–4
[30] Jian L U, Ikehara T, Zhang Y, Mihara1 T, Itoh T and Maeda R 2007 *Japanese Journal of Applied Physics* **46** 7643–7